Hydrol. Earth Syst. Sci. Discuss., 12, 8977–9002, 2015
www.hydrol-earth-syst-sci-discuss.net/12/8977/2015/
doi:10.5194/hessd-12-8977-2015

Hydrology and Earth System Sciences
Discussions
Open Access

Impact of two different types of El Niño events on runoff over the conterminous United States

T. Tang[1], W. Li[1], and G. Sun[2]

[1]Earth and Ocean Sciences, Nicholas School of the Environment, Duke University, Durham, NC 27708, USA
[2]Eastern Forest Environmental Threat Assessment Center, Southern Research Station, United States Department of Agriculture, Forest Service, Raleigh, NC27606, USA

Received: 28 June 2015 – Accepted: 15 August 2015 – Published: 4 September 2015

Correspondence to: W. Li (wenhong.li@duke.edu)

Published by Copernicus Publications on behalf of the European Geosciences Union.

Abstract

The responses of river runoff to shifts of large-scale climatic patterns are of increasing concerns to water resource planners and managers for long-term climate change adaptation. El Niño is one of the most dominant modes of climate variability that is closely linked to hydrologic extremes such as floods and droughts that cause great loss of lives and properties. However, the different impacts of the two types of El Niño-Central Pacific (CP) and Eastern Pacific (EP)-El Niño on runoff across the conterminous US (CONUS) are not well understood. This study characterizes the impacts of the CP- and EP-El Niño on seasonal and annual runoff using observed historical streamflow data from 658 reference gaging stations and NCAR-CCSM4 model. We found that surface runoff responds similarly to the two types of El Niño events in Southeast, Central, South and Western coastal regions, but differently in Northeast (NE), Pacific Northwest (PNW) and West North Central (WNC) climatic zones. Specifically, EP-El Niño events tend to bring above-average runoff in NE, WNC, and PNW throughout the year while CP-El Niño events cause below-than normal runoff in the three regions. Similar findings were also found by analyzing NCAR-CCSM4 model outputs that captured both the CP- and EP-El Niño events representing the best datasets among selected CMIP5 models. The CCSM4 model simulates lower runoff values during CP-El Niño years than those in EP-El Niño in all of the three climatic regions (NE, PNW and WNC) during 1950–1999. In the future (2050–2099), for both types of El Niño years, runoff is projected to increase over the NE and PNW regions, mainly due to increased precipitation (P). In contrast, the increase of future evapotranspiration (ET) is higher than that of future P, leading to a projected decrease in runoff over the WNC region. In addition, model analysis indicates that all of the three regions (NE, PNW and WNC) are projected to have lower runoff values during CP-El Niño years than EP-El Niño. Our study suggests that US water resources may be distributed more unevenly in space and time with more frequent and intense flood and drought events. The findings from this study have important implications to water

resource management at the regional scale. Information generated from this study is useful for water resource planners to anticipate the influence of two different types of El Niño events on droughts and floods across the CONUS.

1 Introduction

El Niño event is a coupled ocean-atmosphere phenomenon, characterized by anomalous sea surface temperature (SST) in the equatorial Pacific Ocean, with periodicity ranging from 2 to 7 years (Trenberth, 1997). Recent studies indicate that there are two different types of El Niño events (Ashok et al., 2007; Kao and Yu, 2009; Kug et al., 2009; Larkin and Harrison, 2005a; Yeh et al., 2009): an eastern-Pacific (EP) and a central-Pacific (CP) type. The EP-El Niño, or the canonical El Niño, has its SST anomaly center located in the eastern equatorial Pacific (Niño 3 region), with a mean duration of about 15 months while the CP-El Niño is characterized with anomalies of surface wind and SST confined in the central Pacific (Niño 4 region) with a mean duration of about 8 months (Kao and Yu, 2009; Mo, 2010). Because of the different convection patterns and atmospheric responses to the EP- and CP-El Niño events, the influences of the two types of El Niño on regional hydroclimate are different (Li et al., 2011; Mo, 2010; Yu and Zou, 2013; Yu et al., 2012). For example, the conventional EP-El Niño events caused a northeast-to-southwest, from positive anomaly to negative anomaly shift in winter temperature across the US whereas the CP-El Niño events led to a northwest-to-southeast shift pattern (Yu et al., 2012); Mo (2010) reported that the ENSO influences on winter precipitation over the Southwest US is strengthening, while the impact on precipitation over the Ohio Valley is weakening for the recent decades due to the occurrence of the CP-El Niño events. During the late 20th century, the EP-El Niño has become less common while the CP-El Niño has become more frequent (Ashok et al., 2007; Kao and Yu, 2009; Kug et al., 2009; Mo, 2010; Yeh et al., 2009). Some recent studies also suggest that the intensity of CP-El Niño events is increasing and the frequency of CP-El Niño will continue to increase in the 21st century (Kim

HESSD
12, 8977–9002, 2015

and Yu, 2012; Lee and McPhaden, 2010). Since El Niño events represent the most dominant mode of climate variability and have crucial implications to the terrestrial hydrological cycles, it is important to examine the different responses of runoff to the two types of El Niño events, hydroclimate and water balances at regional and continental scales.

The regional distributions of runoff are largely controlled by the balances of precipitation (P) and evapotranspiration (ET). Runoff is not only an indicator of water availability, but also plays a key role in the global biogeochemical cycle, transporting large amount of particulates and dissolved minerals as well as nutrients from land to the ocean (Boyer et al., 2006). It is well-known that climate change has great impacts on runoff and water resources worldwide (Dai et al., 2009; Déry and Wood, 2005; Gerten et al., 2008; Lettenmaier et al., 1994; Petrone et al., 2010; Piao et al., 2010; Xu et al., 2010). These climate-induced changes can, sometimes, result in diverse impacts and risks on regional hydrology and water resources (Field et al., 2014). In fact, shifts in runoff pattern has been observed in many regions (Barnett et al., 2005). For example, earlier snowmelt events are observed due to increasing temperature in winter, which will cause a shift in runoff regime from spring to late winter and thus, a runoff decrease in summer (Burn and Elnur, 2002). During the past half century, as the growing population and increasing demand for freshwater, the availability of freshwater is of great concern to water resource managers and policy-makers in a changing climate (Gleick, 2003; Milliman et al., 2008; Oki and Kanae, 2006; Vörösmarty et al., 2000; Xu et al., 2010). A better understanding on the response of runoff to the large-scale climatic patterns, especially to the climatic extremes becomes increasingly important.

Several attempts have been made to investigate the impact of El Niño on runoff over the US (Dracup and Kahya, 1994; Guetter and Georgakakos, 1996; Kahya and Dracup, 1993; Piechota et al., 1997; Twine et al., 2005; Zorn and Waylen, 1997). While these studies are informative, they either focus on only one single river basin or do not categorize the El Niño events into two types. To our best knowledge, the different

HESSD
12, 8977–9002, 2015

impacts of two types of El Niño on runoff over the CONUS have not been carefully examined.

The overall goal of this study is to understand the different impacts of the two types of El Niño events on regional runoff over the CONUS. We used both measured streamflow data and long-term CMIP5 modelling output to examine the spatial patterns of hydrologic response to the two different El Niño events. Section 2 describes the data and methods used in this study. In Sect. 3, we present the main results to contrast the different impacts of the two types of El Niño on runoff. Conclusions are given in Sect. 4.

2 Data and methodology

2.1 Data

In this study, monthly streamflow data (1999–2009) collected at 658 USGS gaging stations were used to examine the effects of El Niño events on watershed runoff (Fig. 1). These reference watersheds have been compiled to represent watersheds with streamflow under conditions minimally influenced by human activities (Falcone et al., 2010). Three primary criteria were used to select reference watersheds: (1) a quantitative index of anthropogenic modification within the watershed based on GIS-derived variables, (2) visual inspection of every stream gage and drainage basin from recent high-resolution imagery and topographic maps, and (3) information about man-made influences from USGS Annual Water Data Reports (Falcone et al., 2010). For detailed information, please refer to Falcone et al. (2010). Additionally, P and ET anomalies during the two types of El Niño years are also examined. NOAA's precipitation reconstruction over land (PREC/L) data (Chen et al., 2002) is used in this study (available at http://www.esrl.noaa.gov/psd/data/gridded/data.precl.html), which is mainly based on gauge observations. ERA-Interim ET data (Dee et al., 2011), obtained from the European Center for Medium-Range Weather Forecasts (ECMWF), is also employed (available at http://apps.ecmwf.int/datasets/). To improve the significance

HESSD
12, 8977–9002, 2015

and robustness of the results from observations, the state-of-the-art global climate models (GCMs) participating in the Coupled Model Intercomparison Project Phase 5 (CMIP5) (Taylor et al., 2012) are employed. Eight models, including NCAR-CCSM4, CNRM-CM5, GISS-E2H, GFDL-CM2.1, GFDL-ESM-2G, GFDL-ESM-2M, MPI-ESM-LR and Nor-ESM1-M, are selected based on the studies of Mo (2010) and Kim and Yu (2012), because these model output are considered the best ones to capture both two types of El Niño in intensity and frequency. These model outputs are downloaded from ESGF website (http://pcmdi9.llnl.gov/esgf-web-fe/), including both historical and RCP4.5. All of the grid data are re-gridded into the resolution of 0.5° × 0.5°.

2.2 Methods

A composite method is employed in this study to highlight the common features of runoff, *P*, and ET during the EP- and CP-El Niño events. The life cycle of El Niño is based on the definition of Trenberth (1997), starting from June–July–August (JJA) to September–October–November (SON), December–January–February (DJF) and March–April–May (MAM) in the following year. The observed historical El Niño years are referred to the Table 1 of Yu et al. (2012). There are four CP-El Niño events and two EP-El Niño events during the study period. The Monte Carlo technique is used to test the statistical significance.

For CMIP5 models, EP- and CP-El Niño events are defined using SST anomalies (SSTAs) over the Niño 3 (150–90° W, 5° N–5° S) and Niño 4 (160° E–150° W, 5° N–5° S) regions, respectively, following Yeh et al. (2009). Specifically, if the 3-month running mean of SSTA over Niño 3 regions is larger than 0.5° for at least 5 consecutive months and also larger than that of Niño 4 region, this year is defined as an EP-El Niño year. Conversely, if the SSTA over Niño 4 region is higher than 0.5° and larger than that of Niño 3 region, the year will be defined as CP-El Niño year.

HESSD
12, 8977–9002, 2015

3 Results

3.1 Annual runoff composite

Figure 2 shows the composite of annual runoff anomaly during CP- and EP-El Niño years. In the conterminous US, more gaging stations show negative anomalies during CP-El Niño years whereas more stations show positive anomalies during EP-El Niño years. Specifically, during CP-El Niño years (Fig. 2a), significant below-average runoff was observed in the whole Northern US, with extremely dry conditions of up to $-180\,\mathrm{mm\,yr^{-1}}$ (−31 %) in Northeast (NE) and (−11 %) Pacific Northwest (PNW) regions. Above-average runoff is mainly found in the Southern US, with wettest conditions of up to $180\,\mathrm{mm\,yr^{-1}}$ in the Gulf of Mexico. During EP-El Niño years (Fig. 2b), positive anomalies are scattered throughout coastal regions, such as NE, Southeast (SE), West, PNW and western portion of West North Central (WNC) while negative anomalies are mainly observed in inland areas, especially in Central and Upper Midwest regions. In addition, comparing Fig. 2a with Fig. 2b, we found that the responses of runoff to the two types of El Niño are similar in the SE, Western and Central areas, but different in NE, PNW, and western portion of WNC, which are enclosed by dark blue rectangles in Fig. 2 based on the climate zones of NOAA (Karl and Koss, 1984). We will focus the three climate regions that have different response signals during CP- and EP-El Niño years.

Since water resource planners are concerned with runoff variations in each water resource region (WRR) (Seaber et al., 1987), the response of domain averaged runoff to CP- and EP-El Niño events are calculated separately in the 18 WRRs, along with the domain averaged runoff anomalies at the NE, PNW, and WNC climate zones (Fig. 3). During CP (EP)-El Niño years, negative (positive) runoff anomalies are observed in all of the three climatic regions (Fig. 3a). Specifically, for the NE region (37–49° N, 65–80° W), the runoff anomalies are −47 and $94\,\mathrm{mm\,yr^{-1}}$ during CP- and EP-El Niño years, respectively. For the PNW (40–49° N, 116–125° W) and WNC (37–49° N, 104–116° W) regions, they are −148 and $148\,\mathrm{mm\,yr^{-1}}$, and −61 and $54\,\mathrm{mm\,yr^{-1}}$, respectively during

CP- and EP-El Niño years. Among the three regions, PNW has the greatest runoff anomaly values, indicating its relatively high sensitivity of annual mean discharges to El Niño events. Figure 3b illustrates the runoff variations for the 18 WRRs during CP- and EP-El Niño years. Among the 18 WRRs, eight regions have the similar responses to the two types of El Niño, i.e, WRR 3, 12, and 18 are characterized by positive anomalies, while WRR 4, 7, 9, 10, and 11, are featured with negative anomalies. There are 10 WRRs producing different responses to the two types of El Niño, with six regions showing dry condition in CP-El Niño and wet condition in EP-El Niño and four regions showing the opposite response. During CP-El Niño years, 11 out of 18 WRRs (61 %) display negative runoff anomaly compared to 9 WRRs (50 %) during EP-El Niño years. All of the WRRs in the NE, PNW, and WNC areas show dry condition in CP-El Niño years and wet condition in EP-El Niño years, including region 1, 2, 5, 14, 16, and 17. These analyses further reveal that CP-El Niño events tend to bring drier conditions than EP-El Niño events over the CONUS, in agreement with our composite results according to the NOAA climate zones (Fig. 2). It is also found that WRR regions 8, 13, and 15 have positive runoff anomalies during CP-El Niño years and negative anomalies in EP-El Niño years; the different results may need further study considering their relatively scarcity of the gage stations in these WRR regions.

3.2 Seasonal composite

El Niño usually develops in boreal summer and fall, peaks in winter, and decays in spring (Trenberth, 1997). In order to further examine the different impacts of the two types of El Niño on runoff at seasonal time scales, seasonal composite analyses are also performed (Fig. 4), focusing on the three climatic zones first, followed by the 18 WRRs.

HESSD
12, 8977–9002, 2015

3.2.1 NOAA climate regions

During CP-El Niño years, significant negative runoff anomalies are found in all of the NE, PNW, and WNC climate regions throughout the year (Fig. 4, left panels). The driest condition occurs in the PNW, NE, and parts of Ohio Valley, with anomalies of up to −45 mm per season (−10 % ∼ −30 %). The negative anomalies in other regions are relatively small, except for WNC area in JJA. The dry condition is most pronounced in boreal spring (MAM). On the other hand, significant positive anomalies are mainly observed in SE US in JJA. The wetter than normal conditions extend both northeastward and westward and peak in DJF and MAM. This is possibly due to high precipitation in boreal winter and spring brought by CP-El Niño (Larkin and Harrison, 2005b; Mo, 2010).

During EP-El Niño events (Fig. 4, right panels), NE, PNW, and WNC regions are characterized by positive runoff anomalies throughout the year, although NE and PNW show some exceptions (negative runoff anomalies) in DJF. The above than normal runoff can also be observed in other climate regions such as in SE during DJF and MAM, West coast during DJF. The large negative anomalies are mainly restricted in the Upper Midwest, Central and Southern US in JJA, SON, and MAM.

In summary, seasonal composite results are consistent with annual composite analyses, especially for the NE, PNW, and WNC regions, despite their peak runoff values in different seasons.

3.2.2 WRRs

Figure 5 illustrates the seasonal runoff responses to the two types of El Niño for the 18 WRRs. Generally speaking, the seasonal composite results are consistent with annual results (Fig. 3b). During CP-El Niño years, 67 % (12 out of 18), 56 % (10 out of 18), 50 % (9 out of 18) and 56 % (10 out of 18) WRRs show negative runoff anomalies in JJA, SON, DJF and MAM, respectively, indicating that the dry conditions prevail during CP-El Niño years on seasonal scales. Meanwhile, during EP-El Niño years, 56 % (10 out of 18), 50 % (9 out of 18), 61 % (11 out of 18) and 44 % (8 out of 18) WRRs show positive runoff anomalies throughout the four seasons, which reveals a relatively wetter condition in EP-El Niño years. The runoff anomalies of WRRs in each season mirror the evolution of both CP- or EP-El Niño intensities at seasonal scales. For instance, WRR 2 has relative low runoff anomalies in boreal summer (JJA) and fall (SON) during EP-El Niño. However, the runoff anomalies are higher in winter (DJF) and peak in spring (MAM), which is consistent with the life cycle of EP-El Niño events. In conclusion, similar to the three climate regions (NE, PNW, and WNC), the 18 WRRs show the similar responses on seasonal scales as those on annual scales throughout El Niño years, despite some exceptions. For example, WRR 1, in the NE climate zone, shows negative runoff anomalies during CP-El Niño years and positive anomalies during EP-El Niño years for three seasons – JJA, SON and MAM, but in DJF, WRR 1 shows a negative runoff anomaly. This is also the same case for WRR 5, 14, 16 and 17, although with exceptions occur in different seasons.

3.3 Modeled runoff composite

In order to enhance the robustness of our observational results, the same composite is performed to the selected CMIP5 model output, which include more El Niño events. The El Niño years for each model were determined by the methods described in Sect. 2.2. Previous studies suggested that different identification methods may lead to slight differences in the number of El Niño years (Yu and Kim, 2013; Yu et al., 2012). Nonetheless, such differences in El Niño frequency do not affect the main results (not shown). Pattern correlations are used to evaluate the simulation of runoff for the eight CMIP5 models which reasonably capture the two types of El Niño (Kim and Yu, 2012; Mo, 2010). All of the eight model outputs have a pattern correlation over 0.8 in simulating the long-term mean monthly runoff. In simulating the response of runoff to the two types of El Niño, NCAR-CCSM4 model is identified as the best model with the highest pattern correlation (Table 1 and Fig. 6). The main features of El Niño impacts on runoff are clearly reproduced. For example, during CP-El Niño years

HESSD
12, 8977–9002, 2015

(Fig. 6a), the dry conditions in NE, Ohio Valley, WNC, and PNW, and wet conditions in SE, West and Southwest (SW) are simulated quite well. For EP-El Niño (Fig. 6b), the runoff anomalies are mainly characterized by wet conditions except for Ohio Valley and some parts of Pacific Northwest (PNW), in consistent with observations (Fig. 2). The model results further enhanced the robustness of composite results from observations, despite some slight differences (Figs. 2, 6). In summary, both observational results and model simulations reveal that the responses of runoff to the two types of El Niño are similar in SE, SW, and Western coastal areas, but different in NE, PNW, and WNC regions.

3.4 Water balance

3.4.1 Observations

In order to further understand the response of runoff to El Niño in light of water balance, the composites of P and ET are also performed (Fig. 7). In the long term, such as the time scale in the study (Brubaker et al., 1993), for a large watershed, runoff is mainly controlled by P and ET (runoff = P – ET). It is shown that, over the CONUS, the runoff anomaly pattern largely follows P anomaly pattern, with pattern correlations of 0.66 and 0.36 in both CP- and EP-El Niño years. For the three climate regions (NE, PNW, and WNC), the P anomalies are all negative during CP-El Niño years, but all positive during EP-El Niño years. The different P anomalies during the two types of El Niño years largely explain the different runoff responses in the three climate regions. Our composite result of P is in agreement with Yu and Zou (2013), who reported a drier condition across the CONUS in CP-El Niño years, which is characterized by less precipitation.

HESSD
12, 8977–9002, 2015

3.4.2 Model output

Current climate data suggest that runoff variations during different El Niño years are largely determined by *P* over the CONUS. In a warming climate, with the increase of temperature and potential ET (PET) (Dai et al., 2010; Lu et al., 2009), whether future runoff anomalies are still dominated by *P* anomalies in the three climate regions (NE, PNW and WNC) is studied by comparing NCAR-CCSM4 model historical and RCP4.5 runs output (Table 2).

For the NE region, the mean annual runoff in CP-El Niño years is about 76 mm lower than that in EP-El Niño years in the current climate (1950–1999) mainly because of a lower *P* (1099 vs 1184 mm) and nearly same ET (Table 2). In the future (2050–2099), runoff, *P*, and ET are projected to increase during both types of El Niño years in this region. However, runoff in CP-El Niño years is about 109 mm lower than that of future EP-El Niño years. The lower runoff is a combined effects of a lower *P* (66 mm), and a higher ET (43 mm) presumably due to an increase of PET as a result of global warming. The similar results are also found in the PNW region: lower runoff during CP-El Niño years than that in EP-El Niño year; an increased future runoff for both CP- and EP-El Niño events associated with increasing future *P*.

In the WNC region, similar to the NE and PNW regions, runoff is about 7 mm lower in CP-El Niño years than that in EP-El Niño years because *P* is 50 mm lower and ET is 43 mm lower in the current climate (Table 2). However, when climate warms in the future, different from the NE and PNW climate zones, surface runoff will decrease by 14 and 5 mm during CP- and EP-El Niño years, respectively. Table 2 indicates that the net increases of ET during the CP- and EP- El Niño years, i.e., 70 and 33 mm, are larger than the increases of *P* (i.e., 56 and 33 mm), leading to decreased future runoff during El Niño events over the region. Such increases of *P* and ET in the future are possibly due to global warming. The average temperature during the two types of El Niño years increases by $\sim 2\,^{\circ}\mathrm{C}$ in the 21st century (RCP4.5), compared with the 20th century. A higher temperature usually leads to a higher PET (Dai et al., 2010; Lu et

HESSD
12, 8977–9002, 2015

al., 2009); when future ET enhancement is greater than the increased P such as in the WNC region during El Niño years, surface runoff will decrease.

In summary, runoff value during CP-El Niño years is lower than that during EP-El Niño years, indicating a drier condition in all three climate regions during both current and future climate. In the future when climate warms, CCSM4 model suggests that surface runoff will increase in the NE and PNW regions during the two types of El Niño, largely due to an increase of future P; however, over the WNC, runoff is likely to decrease because the increase of ET is much higher than P increase for both El Niño events. Our analyses reveal that changes in ET due to global warming would play a more important role in altering surface discharge for some regions.

4 Conclusions

The different impacts of CP- and EP-El Niño events as extreme climate on surface runoff over the CONUS was studied using 658 gaging stations and NCAR-CCSM4 model output. It is shown that surface runoff responds similarly to the two types of El Niño events in Southeast, Central, South and Western coastal regions, but differently in NE, PNW, and WNC states. In general, the CP-El Niño events are likely to cause dry conditions with lower runoff whereas the EP-El Niño events tend to result in wetter than normal conditions over CONUS. This can also be seen from the runoff responses at the 18 WRRs. Such runoff anomalies are largely following the variation of P during El Niño years. The NCAR-CCSM4 model outputs further support the conclusions from observation, i.e., a drier condition over the CONUS during CP-El Niño years than EP-El Niño. It is also projected that future runoff tend to decrease over the WNC region whereas increase over the NW and PNE regions during both types of El Niño events. The former is associated with a greater increase in ET amount vs P in a warmer climate, while the latter is the opposite. These results suggest that surface water resources may be distributed more unevenly in space and time in the future El Niño years. Such information is useful to develop plans in anticipating hydrologic extremes under future climate change.

HESSD
12, 8977–9002, 2015

Acknowledgements. We would like to thank USGS for providing runoff data, NOAA for providing land precipitation data, and ECMWF for providing ERA-Interim ET data, as well as ESGF portal for providing CMIP5 global climate model output. This study is partially supported by the National Science Foundation Grant AGS-1147608, and the Eastern Forest Environmental Threat Assessment Center, Southern Research Station, U.S. Department of Agriculture, Forest Service.

References

Ashok, K., Behera, S. K., Rao, S. A., Weng, H., and Yamagata, T.: El Niño Modoki and its possible teleconnection, J. Geophys. Res., 112, C11007, doi:10.1029/2006JC003798, 2007.

Barnett, T. P., Adam, J. C., and Lettenmaier, D. P.: Potential impacts of a warming climate on water availability in snow-dominated regions, Nature, 438, 303–309, doi:10.1038/nature04141, 2005.

Boyer, E. W., Howarth, R. W., Galloway, J. N., Dentener, F. J., Green, P. A., and Vörösmarty, C. J.: Riverine nitrogen export from the continents to the coasts, Global Biogeochem. Cy., 20, GB1S91, doi:10.1029/2005GB002537, 2006.

Brubaker, K. L., Entekhabi, D., and Eagleson, P.: Estimation of continental precipitation recycling, J. Climate, 6, 1077–1089, doi:10.1175/1520-0442(1993)006< 1077:EOCPR> 2.0.CO;2, 1993.

Burn, D. H. and Elnur, M. A. H.: Detection of hydrologic trends and variability, J. Hydrol., 255, 107–122, doi:10.1016/S0022-1694(01)00514-5, 2002.

Chen, M., Xie, P., Janowiak, J. E., and Arkin, P. A.: Global land precipitation: A 50-yr monthly analysis based on gauge observations, J. Hydrometeorol., 3, 249–266, doi:10.1175/1525-7541(2002)003<0249:GLPAYM> 2.0.CO;2, 2002.

Dai, A., Qian, T., Trenberth, K. E., and Milliman, J. D.: Changes in continental freshwater discharge from 1948 to 2004, J. Climate, 22, 2773–2792, doi:10.1175/2008JCLI2592.1, 2009.

Dai, Z., Trettin, C. C., Li, C., Amatya, D. M., Sun, G., and Li, H.: Sensitivity of Stream flow and Water Table Depth to Potential Climatic Variability in a Coastal Forested Watershed, J. Am. Water Resour. As. (JAWRA), 46, 1036–1048, doi:10.1111/j.1752-1688.2010.00474.x, 2010.

Dee, D. P., Uppala, S. M., Simmons, A. J., Berrisford, P., Poli, P., Kobayashi, S., Andrae, U., Balmaseda, M. A., Balsamo, G., Bauer, P., Bechtold, P., Beljaars, A. C. M., van de Berg, L., Bidlot, J., Bormann, N., Delsol, C., Dragani, R., Fuentes, M., Geer, A. J., Haimberger, L., Healy, S. B., Hersbach, H., Hólm, E. V., Isaksen, L., Kållberg, P., Köhler, M., Matricardi, M., McNally, A. P., Monge-Sanz, B. M., Morcrette, J.-J., Park, B.-K., Peubey, C., de Rosnay, P., Tavolato, C., Thépaut, J.-N., and Vitart, F.: The ERA-Interim reanalysis: Configuration and performance of the data assimilation system, Q. J. Roy. Meteor. Soc., 137, 553–597, doi:10.1002/qj.828, 2011.

Déry, S. J. and Wood, E.: Decreasing river discharge in northern Canada, Geophys. Res. Lett., 32, L10401, doi:10.1029/2005GL022845, 2005.

Dracup, J. A. and Kahya, E.: The relationships between US streamflow and La Niña events, Water Resour. Res., 30, 2133–2141, doi:10.1029/94WR00751, 1994.

Falcone, J. A., Carlisle, D. M., Wolock, D. M., and Meador, M. R.: GAGES: a stream gage database for evaluating natural and altered flow conditions in the conterminous United States, Ecology, 91, 621–621, doi:10.1890/09-0889.1, 2010.

Field, C. B., Barros, V. R., Dokken, M. D., et al.: IPCC, 2014: Climate Change 2014: Impacts, Adaptation, and Vulnerability. Part A: Global and Sectoral Aspects. Contribution of Working Group II to the Fifth Assessment Report of the Intergovernmental Panel on Climate Change, edited by: Field, C. B., Barros, V. R., Dokken, D. J., Mach, K. J., Mastrandrea, M. D., Bilir, T. E., Chatterjee, M., Ebi, K. L., Estrada, Y. O., Genova, R. C., Girma, B., Kissel, E. S., Levy, A. N., MacCracken, S., Mastrandrea, P. R., and White, L. L., Cambridge University Press, Cambridge, United Kingdom and New York, NY, USA, 2014.

Gerten, D., Rost, S., von Bloh, W., and Lucht, W.: Causes of change in 20th century global river discharge, Geophys. Res. Lett., 35, L20405, doi:10.1029/2008GL035258, 2008.

Gleick, P. H.: Global freshwater resources: soft-path solutions for the 21st century, Science, 302, 1524-1528, doi:10.1126/science.1089967, 2003.

Guetter, A. K. and Georgakakos, K. P.: Are the El Niño and La Niña predictors of the Iowa River seasonal flow?, J. Appl. Meteorol., 35, 690–705, doi:10.1175/1520-0450(1996)035<0690:ATENAL>2.0.CO;2, 1996.

Kahya, E. and Dracup, J. A.: US streamflow patterns in relation to the El Niño/Southern Oscillation, Water Resour. Res., 29, 2491–2503, doi:10.1029/93WR00744, 1993

Kao, H.-Y. and Yu, J.-Y.: Contrasting eastern-Pacific and central-Pacific types of ENSO, J. Climate, 22, 615–632, doi:10.1175/2008JCLI2309.1, 2009.

HESSD

12, 8977–9002, 2015

Title Page

Abstract | Introduction

Conclusions | References

Tables | Figures

◀| |▶

◀ ▶

Back | Close

Full Screen / Esc

Printer-friendly Version

Interactive Discussion

Karl, T. and Koss, W. J.: Regional and National Monthly, Seasonal, and Annual Temperature Weighted by Area, 1895–1983, National Climatic Data Center, Asheville, NC, 1984.
Kim, S. T. and Yu, J. Y.: The two types of ENSO in CMIP5 models, Geophys. Res. Lett., 39, L11704, doi:10.1029/2012GL052006, 2012.
Kug, J.-S., Jin, F.-F., and An, S.-I.: Two types of El Niño events: cold tongue El Niño and warm pool El Niño, J. Climate, 22, 1499–1515, doi:10.1175/2008JCLI2624.1, 2009.
Larkin, N. K. and Harrison, D.: Global seasonal temperature and precipitation anomalies during El Niño autumn and winter, Geophys. Res. Lett., 32, L16705, doi:10.1029/2005GL022860, 2005a.
Larkin, N. K. and Harrison, D.: On the definition of El Niño and associated seasonal average US weather anomalies, Geophys. Res. Lett., 32, L13705, doi:10.1029/2005GL022738, 2005b.
Lee, T. and McPhaden, M. J.: Increasing intensity of El Niño in the central-equatorial Pacific, Geophys. Res. Lett., 37, L14603, doi:10.1029/2010GL044007, 2010.
Lettenmaier, D. P., Wood, E. F., and Wallis, J. R.: Hydro-climatological trends in the continental United States, 1948–88, J. Climate, 7, 586–607, doi:10.1175/1520-0442(1994)007< 0586:HCTITC> 2.0.CO;2, 1994.
Li, W., Zhang, P., Ye, J., Li, L., and Baker, P. A.: Impact of two different types of El Niño events on the Amazon climate and ecosystem productivity, J. Plant Ecol., 4, 91–99, doi:10.1093/jpe/rtq039, 2011.
Lu, J., Sun, G., McNulty, S. G., and Comerford, N. B.: Sensitivity of pine flatwoods hydrology to climate change and forest management in Florida, USA, Wetlands, 29, 826–836, doi:10.1672/07-162.1, 2009.
Milliman, J., Farnsworth, K., Jones, P., Xu, K., and Smith, L.: Climatic and anthropogenic factors affecting river discharge to the global ocean, 1951–2000, Global Planet. Change, 62, 187–194, doi:10.1016/j.gloplacha.2008.03.001, 2008.
Mo, K. C.: Interdecadal modulation of the impact of ENSO on precipitation and temperature over the United States, J. Climate, 23, 3639–3656, doi:10.1175/2010JCLI3553.1, 2010.
Oki, T. and Kanae, S.: Global hydrological cycles and world water resources, Science, 313, 1068–1072, doi:10.1126/science.1128845, 2006.
Petrone, K. C., Hughes, J. D., Van Niel, T. G., and Silberstein, R. P.: Streamflow decline in southwestern Australia, 1950–2008, Geophys. Res. Lett., 37, L11401, doi:10.1029/2010GL043102, 2010.

Piao, S., Ciais, P., Huang, Y., Shen, Z., Peng, S., Li, J., Zhou, L., Liu, H., Ma, Y., Ding, Y., Friedlingstein, P., Liu, C., Tan, K., Yu, Y., Zhang, T., and Fang, J.: The impacts of climate change on water resources and agriculture in China, Nature, 467, 43–51, doi:10.1038/nature09364, 2010.

Piechota, T. C., Dracup, J. A., and Fovell, R. G.: Western US streamflow and atmospheric circulation patterns during El Niño-Southern Oscillation, J. Hydrol., 201, 249–271, doi:10.1016/S0022-1694(97)00043-7, 1997.

Seaber, P. R., Kapinos, F. P., and Knapp, G. L.: Hydrologic unit maps, US Government Printing Office, Washington, DC 20401, 1987.

Taylor, K. E., Stouffer, R. J., and Meehl, G. A.: An overview of CMIP5 and the experiment design, B. Am. Meteorol. Soc., 93, 485–498, doi:10.1175/BAMS-D-11-00094.1, 2012.

Trenberth, K. E.: The definition of El Nino, B. Am. Meteorol. Soc., 78, 2771–2777, doi:10.1175/1520-0477(1997)078< 2771:TDOENO>2.0.CO;2, 1997.

Twine, T. E., Kucharik, C. J., and Foley, J. A.: Effects of El Nino-Southern Oscillation on the climate, water balance, and streamflow of the Mississippi River basin, J. Climate, 18, 4840–4861, doi:10.1175/JCLI3566.1, 2005.

Vörösmarty, C. J., Green, P., Salisbury, J., and Lammers, R. B.: Global water resources: vulnerability from climate change and population growth, Science, 289, 284–288, doi:10.1126/science.289.5477.284, 2000.

Xu, K., Milliman, J. D., and Xu, H.: Temporal trend of precipitation and runoff in major Chinese Rivers since 1951, Global Planet. Change, 73, 219–232, doi:10.1016/j.gloplacha.2010.07.002, 2010.

Yeh, S.-W., Kug, J.-S., Dewitte, B., Kwon, M.-H., Kirtman, B. P., and Jin, F.-F.: El Niño in a changing climate, Nature, 461, 511–514, doi:10.1038/nature08316, 2009.

Yu, J.-Y. and Zou, Y.: The enhanced drying effect of Central-Pacific El Niño on US winter, Environ. Res. Lett., 8, 014019, doi:10.1088/1748-9326/8/1/014019, 2013.

Yu, J. Y. and Kim, S. T.: Identifying the types of major El Niño events since 1870, Int. J. Climatol., 33, 2105–2112, doi:10.1002/joc.3575, 2013.

Yu, J. Y., Zou, Y., Kim, S. T., and Lee, T.: The changing impact of El Niño on US winter temperatures, Geophys. Res. Lett., 39, L15702, doi:10.1029/2012GL052483, 2012.

Zorn, M. R. and Waylen, P. R.: Seasonal response of mean monthly streamflow to El Nino/Southern Oscillation in north central Florida, The Professional Geographer, 49, 51–62, doi:10.1111/0033-0124.00055, 1997.

HESSD

12, 8977–9002, 2015

Impact of El Niño on runoff across the US

T. Tang et al.

Table 1. Pattern correlations of runoff for the selected models.

	CP	EP
NCAR-CCSM4	0.42	0.28
NASA-GISS-E2H	0.42	0.18
CNRM-CM5	0.34	−0.06
GFDL-CM2.1	0.50	−0.015
GFDL-ESM-2G	0.16	0.09
GFDL-ESM-2M	0.28	0.11
MPI-ESM-LR	−0.21	−0.34
Nor-ESM1-M	−0.07	−0.008

HESSD
12, 8977–9002, 2015

Table 2. Mean annual runoff, P, and ET over the three climate regions during two different types of El Niño years based on the NCAR-CCSM4 model historical and future simulations (unit: mm).

	Historical (1950–1999)			RCP45 (2050–2099)		
	Runoff	P	ET	Runoff	P	ET
Northeast						
CP-El Niño	418	1099	681	457	1185	728
EP-El Niño	494	1184	690	566	1251	685
Climatology mean	459	1135	676	505	1215	710
Pacific Northwest						
CP-El Niño	562	1050	488	626	1160	534
EP-El Niño	630	1149	519	665	1181	516
Climatology mean	611	1099	488	634	1144	510
West North Central						
CP-El Niño	161	655	494	147	711	564
EP-El Niño	168	705	537	163	733	570
Climatology mean	166	664	498	158	691	533

HESSD
12, 8977–9002, 2015

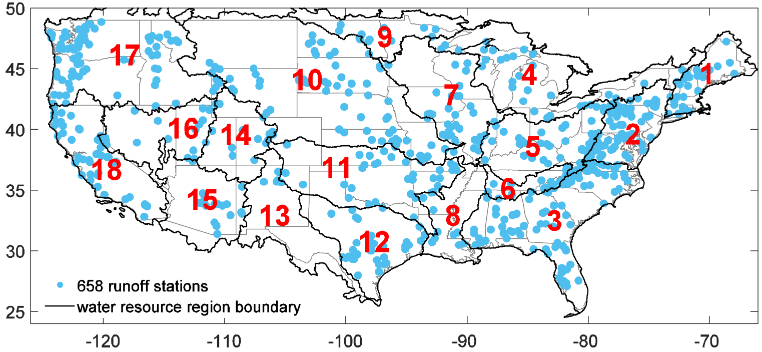

Figure 1. 658 gaging stations (blue dots) and the 18 water resource regions defined by USGS over the CONUS.

HESSD
12, 8977–9002, 2015

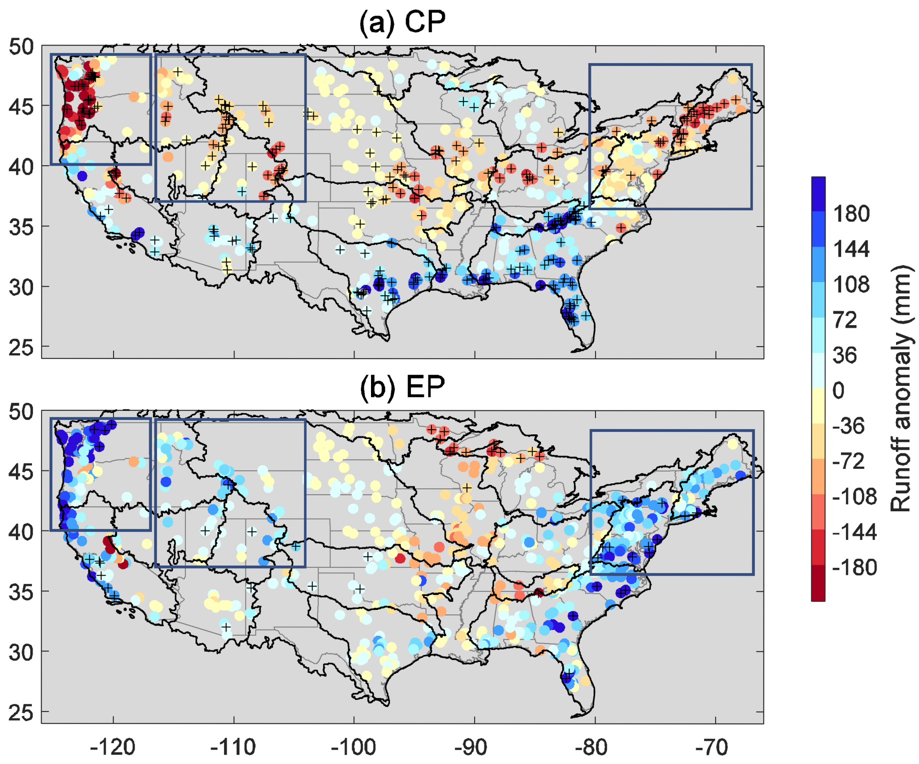

Figure 2. Composite of annual runoff anomaly (unit: mm) for the two types of El Niño during the period of 1990–2009 **(a)** in CP-El Niño years; **(b)** in EP-El Niño years. + indicates results at 0.05 significance level based on Monte Carlo test. Three climate regions (NE, PNW, and WNC) and 18 WRRs are plotted using blue rectangles and dark black lines, respectively.

HESSD
12, 8977–9002, 2015

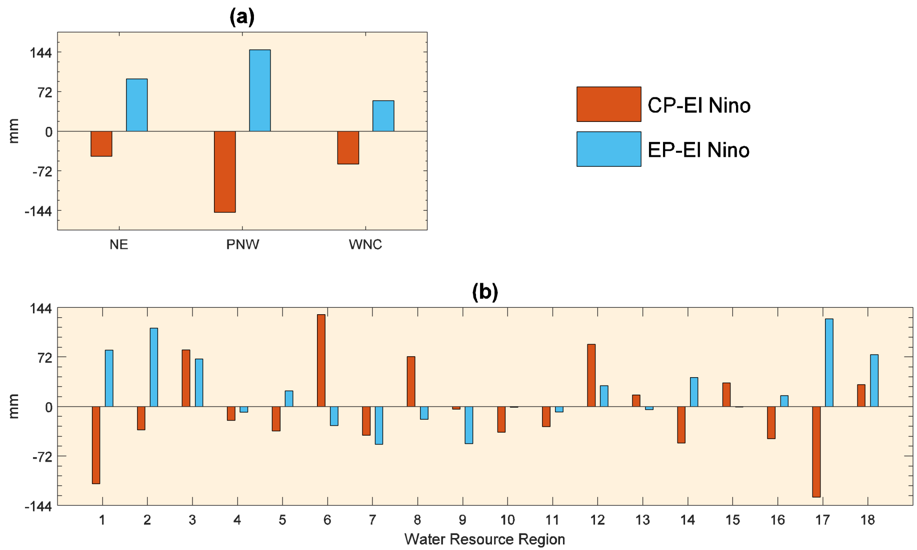

Figure 3. Domain averaged annual runoff anomalies (unit: mm) for **(a)** NE, PNW, and WNC climate regions; **(b)** the 18 WRRs, during CP- and EP-El Niño years.

HESSD
12, 8977–9002, 2015

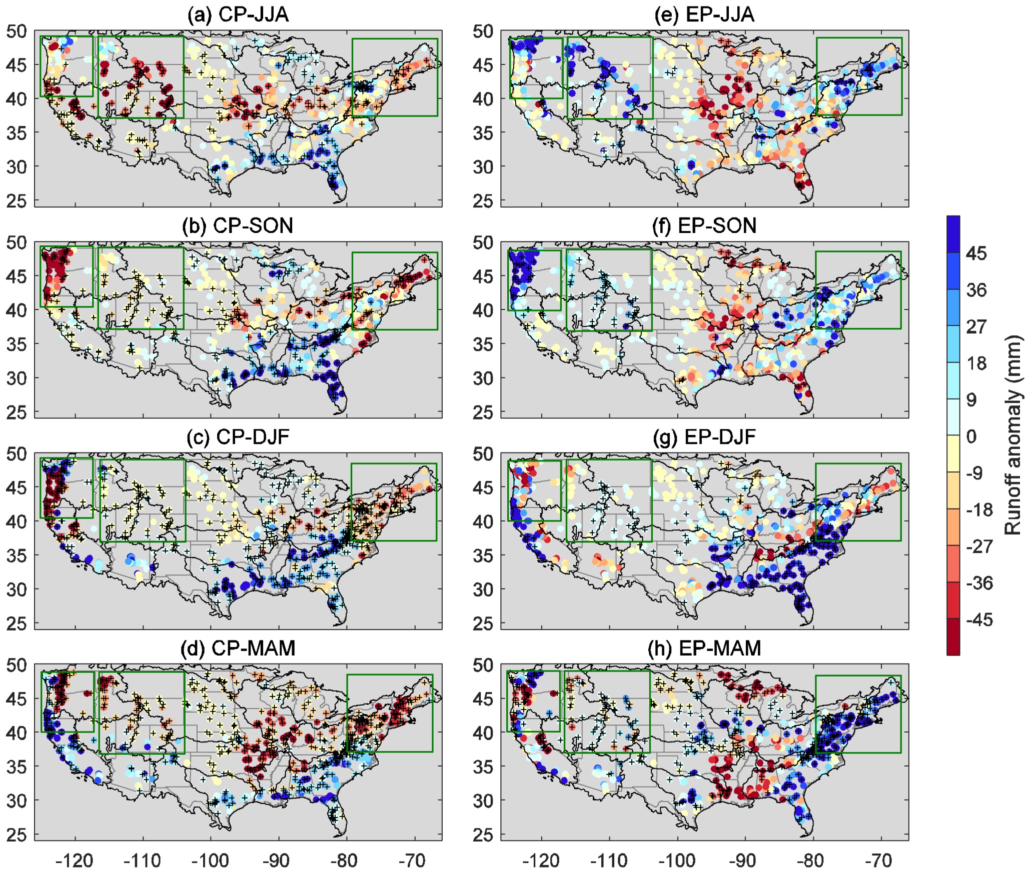

Figure 4. Seasonal composite of runoff anomaly (unit: mm) for the two types of El Niño on **(a)** JJA, **(b)** SON, **(c)** DJF, and **(d)** MAM in CP-El Niño years during the period of 1990–2009; **(e–h)** the same as **(a–d)**, but for EP-El Niño years. + indicates results at 0.05 significance level based on Monte Carlo test.

HESSD
12, 8977–9002, 2015

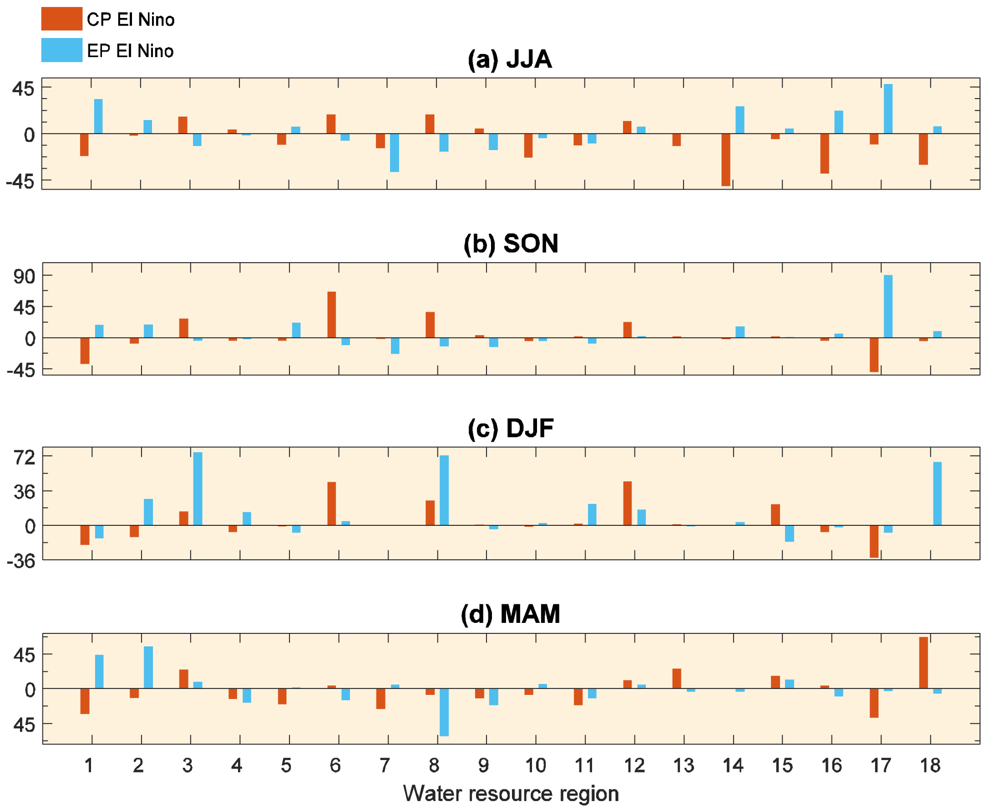

Figure 5. Seasonal domain averaged runoff anomalies (unit: mm) for the 18 WRRs at **(a)** JJA, **(b)** SON, **(c)** DJF, and **(d)** MAM during CP- and EP-El Niño years.

HESSD
12, 8977–9002, 2015
Impact of El Niño on runoff across the US
T. Tang et al.

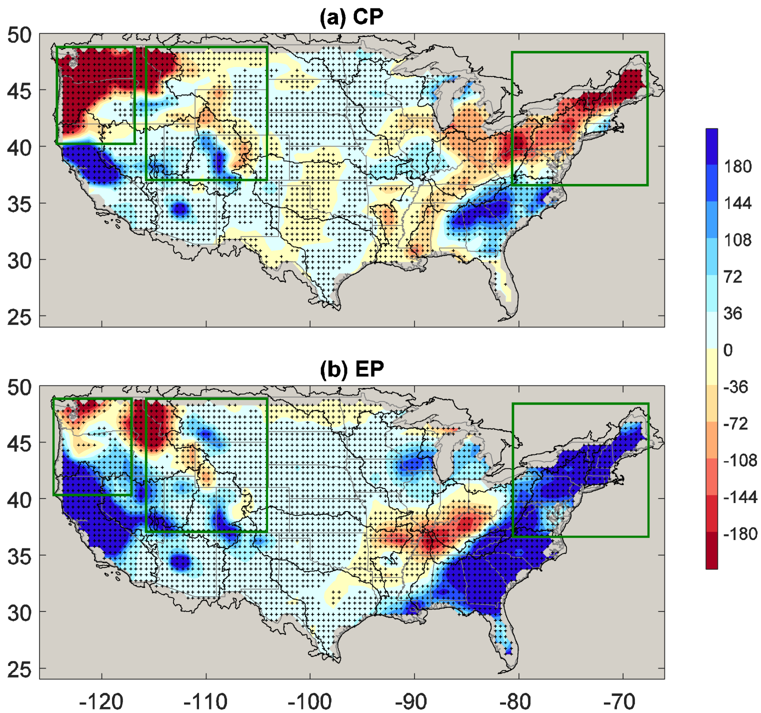

Figure 6. Same as Fig. 2, but using NCAR-CCSM4 model historical output (unit: mm).

HESSD
12, 8977–9002, 2015

Impact of El Niño on runoff across the US

T. Tang et al.

Title Page
Abstract
Introduction
Conclusions
References
Tables
Figures
◀
▶
Back
Close
Full Screen / Esc
Printer-friendly Version
Interactive Discussion

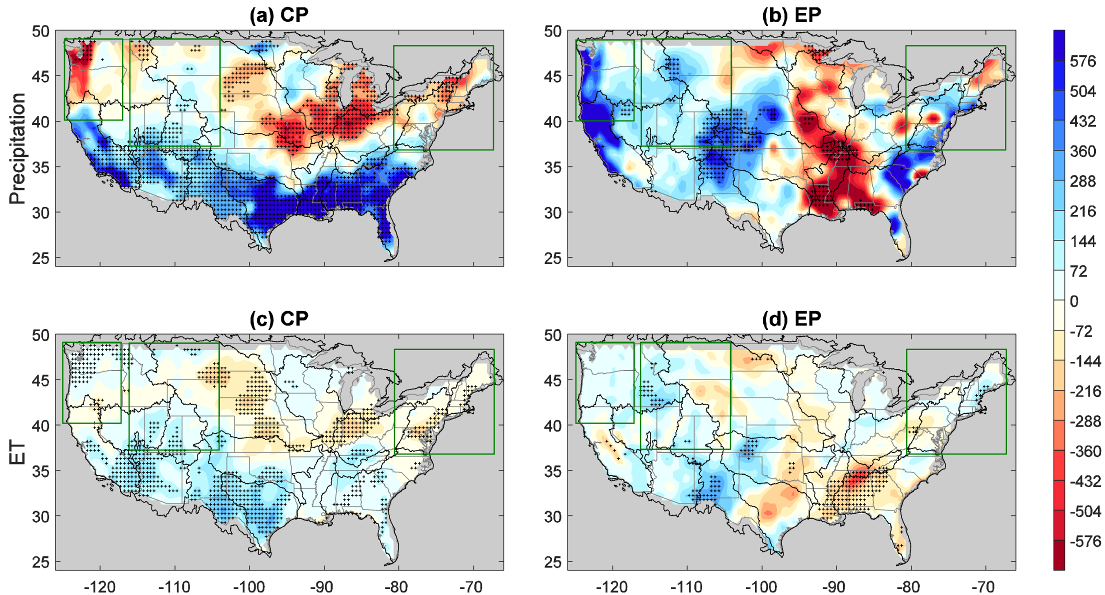

Figure 7. Same as Fig. 2, but for precipitation (**a** and **b**) and evapotranspiration (**c** and **d**) during CP- and EP-El Nino events (unit: mm).